Low-Cost Heaving Single-Buoy Wave-Energy Point Absorber Optimization for Sardinia West Coast

Journal of *Marine Science and Engineering*

MDPI

Article

Low-Cost Heaving Single-Buoy Wave-Energy Point Absorber Optimization for Sardinia West Coast

Marcello Rava [1,2,*], Panagiotis Dafnakis [1], Vittorio Martini [2], Giuseppe Giorgi [1], Vincenzo Orlando [2], Giuliana Mattiazzo [1], Giovanni Bracco [1] and Andrea Gulisano [2]

[1] Marine Offshore Renewable Energy Lab (MOREnergy Lab), Department of Mechanical and Aerospace Engineering (DIMEAS), Politecnico di Torino, 10129 Turin, Italy; panagiotis.dafnakis@polito.it (P.D.); giuseppe.giorgi@polito.it (G.G.); giuliana.mattiazzo@polito.it (G.M.); giovanni.bracco@polito.it (G.B.)

[2] Wave for Energy S.r.l., 10129 Turin, Italy; v.martini@waveforenergy.com (V.M.); v.orlando@waveforenergy.com (V.O.); a.gulisano@waveforenergy.com (A.G.)

* Correspondence: marcello.rava@polito.it

Abstract: This work presents the Water Energy Point Absorber (WEPA), which is a heaving single-buoy point absorber optimized for a specific site off the west coast of Sardinia Island. The aim of the study is to present the optimization process undertaken to identify the best configuration in terms of performance and cost. The optimization is carried out thanks to a simulation tool developed in Matlab-Simulink environment and verified through to the commercial software Orcaflex. Simulations are performed in the time domain with the installation site's waves as input. The hydrodynamics parameters are computed thanks to the commercial software Ansys Aqwa and given to the model as input. The yearly energy production is computed as output for each configuration. Several parametric analyses are performed to identify the optimal Power Take Off (PTO) and buoy size. Among the main findings, it shall be mentioned that the PTO-rated torque has a strong influence on the energy production, higher PTO-rated torque proved to have better performance. The optimal hull size is strictly related to the incoming waves, and for the given site the smaller hulls are performing better than larger ones. The hull height, hull mass and hull draft have little impact on productivity. Finally, a comprehensive techno–economic analysis is performed, showing that the best configuration can be identified only after a detailed feasibility study and rigorous cost analysis.

Keywords: wave-energy conversion; single-buoy point absorber; parametric optimization; time-domain simulations; matlab; simulink; techno–economic analysis

Citation: Rava, M.; Dafnakis, P.; Martini, V.; Giorgi, G.; Orlando, V.; Mattiazzo, G.; Bracco, G.; Gulisano, A. Low-Cost Heaving Single-Buoy Wave-Energy Point Absorber Optimization for Sardinia West Coast. *J. Mar. Sci. Eng.* **2022**, *10*, 397. https://doi.org/10.3390/jmse10030397

Academic Editors: Vincenzo Nava and Markel Penalba

Received: 15 January 2022
Accepted: 19 February 2022
Published: 9 March 2022

1. Introduction

Due to the negative impacts of fossil fuels, great attention has been dedicated to renewable energy sources in the last years. Wave energy is a promising source of clean and abundant energy due to its enormous potential, however, much work still has to be carried out before proving it to be economically competitive. The earliest wave-energy patent was filed in France in 1799 [1], and since then, several others have been submitted along with books and scientific articles. Despite the great scientific effort, to date no wave-energy conversion technology is proven to be commercially ready for large-scale production. One of the greatest challenges is the energy yield estimation in a real sea environment and the associated costs [2]. Estimating Wave Energy Converter (WEC) performances and costs at an early stage of development is crucial to decide whether to drop or further investigate the technology, avoiding money and time waste [3,4]. A cost analysis shall be carried out here, including field information and considering the whole life cycle of the device, from the construction to the end of life. Today, thanks to the increasing computational power and the more advanced mathematical models, helpful simulation tools can be developed to reach optimal solutions for specific wave climates [5,6].

1.1. Objective

The objective of this paper is to present the new single-buoy heaving wave-energy converter, "Water Energy Point Absorber" (WEPA), which is unique in its category. To prove its novelty, a comparison with the most similar existing WEC is provided. Furthermore, this article exposes the methodology used to optimize WEPA for a specific case study. The optimization is performed thanks to a simulation tool developed in matlab-simulink and a parametric study. The parametric optimization study is based on a set of sensitivity analyses on the main WEC's parameters. The optimization process described in this paper fills the gap of current studies as it includes an advanced feasibility study and techno–economic analysis. It is shown that an effective techno–economic optimization can lead to a final design for a given site in a relatively short time.

This work should provide a valuable research contribution to the scientific community and companies operating in the wave-energy field that need to design and build a full-scale prototype, as it provides an optimization process applied on a real case study including a techno–economic analysis.

1.2. Wepa Concept

The wave-energy converter described in this paper is WEPA, which stands for "Water Energy Point Absorber". It has the main objective of producing electricity and freshwater from desalination. It has been developed thanks to the experience that Politecnico di Torino and its spin-off company, Wave for Energy, have gained in recent years in the offshore energy sector, in particular, thanks to the Inertial Sea Wave Energy Converter (ISWEC) development [7,8]. The WEPA architecture is simplified to the maximum extent to increase reliability and reduce maintenance. The goal is to drastically reduce the costs in order to reach economic sustainability and marketability in the shortest possible time.

The working principle of WEPA is efficient and straightforward—it harvests energy from the relative motion between the buoy and the seabed. Most of the energy is extracted from the buoy heaving motions, however, motions on other degrees of freedom can also marginally contribute to the energy production. The production tether is fixed to the seabed on one side and is wrapped around a grooved drum inside the hull on the other side. The tether is made out of a highly rigid fiber rope and it enters inside the hull in the central bottom part. As can be seen in Figure 1, each time the buoy climbs up to the wave crest, moving with positive velocity (from STEP 1 to STEP 3), the tether is unwinding and the drum is forced to rotate. While each time the buoy slopes down in the wave trough, moving with negative velocity (from STEP 3 to STEP 5), the tether is winding around the drum thanks to a spiral spring or the generator used as a motor.

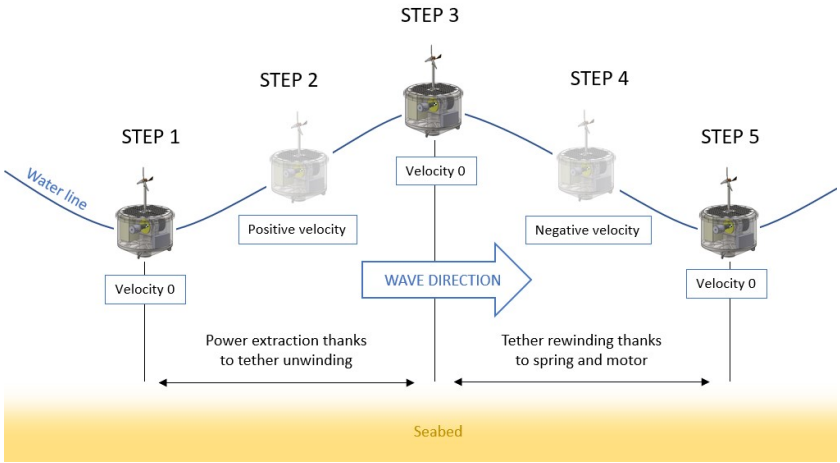

Figure 1. WEPA working principle.

The grooved drum is directly connected to the generator and the spiral spring forming the Power Take Off (PTO) system. As shown in Figure 2, the grooved drum is located in a channel open to the sea on the lower side, and this allows the tether to enter the hull. The spring is connected on one side of the drum and the generator is on the other side. Thanks to a sealing system mounted on the shafts on both sides of the drum, the water does not enter the watertight chamber where the electrical and mechanical components are located. Therefore, only the grooved drum and a portion of the shafts are exposed to the harsh sea environment.

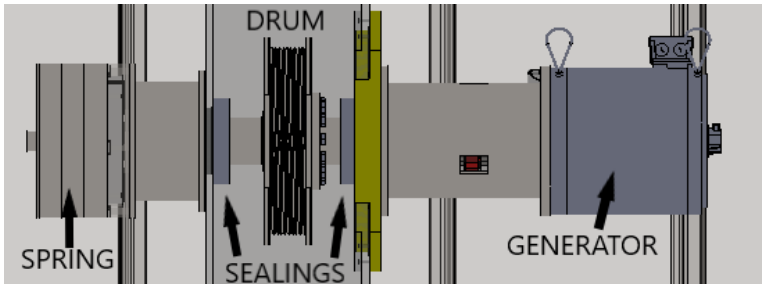

Figure 2. WEPA PTO system.

The generator used for this prototype is a permanent magnet synchronous electrical machine, often referred to as torque motor, due to the low speed and high torque that it can provide thanks to the high number of poles. Several types of PTO have already been tested [9]. For this prototype, a direct-drive electrical generator is used, however, the hydraulic PTO should be tested in further investigations.

To increase energy-conversion efficiency, advanced PTO control strategies shall be implemented, as the passive control strategies (fixed PTO stiffness and damping) have shown poor performances [10]. Thanks to PTO damping tuning, WEPA can adapt its behaviour to the wave climate to maximize energy extraction.

Point absorbers in general, and WEPA in particular, are expected to be deployed in arrays of several units to create wave farms [11]. This modularity feature helps reduce costs, and thus, increases WEPA competitiveness. However, hydrodynamic interactions shall be carefully studied to avoid power losses.

The environmental impact of the entire life cycle of a WEC shall be studied towards the end of the design, so that all the crucial elements are already defined but eventually some modifications can be performed to reduce the environmental impact (e.g., change from one material to another). According to [12] the greenhouse gas (GHG) emissions of wave energy technologies are very limited, with reference values lower than 50 gCO_2/kWh. Regarding direct environmental impacts, the WEPA mooring system has the advantage of eliminating the portions of the line in contact with the seabed, avoiding seabed erosion. However, a possible impact could be related to the noise of the moving mechanical components located inside the hull.

1.3. Comparison with Existing Wave-Energy Conversion Technologies

Contrarily to wind and solar energy, wave energy is still in an early development phase, in which several different concepts and ideas are being investigated and compared. Some concepts may drastically differ from each other, and therefore categorization can be challenging. However, it can be made according to three main groups differentiated by working principle: terminator, attenuator and point absorber [13–15]. The category "terminator" includes WECs with the larger dimension parallel to the direction of incoming wave, "attenuator" includes WECs with the larger dimension orthogonal to the direction of incoming wave, and finally, category "point absorber", the one to which WEPA belongs, contains all the devices with small dimensions compared to the predominant wavelength of the prevailing waves. Different point absorber configurations have been developed by

research groups and companies, and according to [16], a total of 83 point absorber concepts have been proposed.

Among the companies that have developed heaving single-buoy point absorbers can be found SeaBased, which has developed and tested several WECs. They use a fixed reference point at the seabed, where the PTO, a linear generator, is also placed [17]. The PTO is connected to the floater thanks to a mooring line; the floater is an empty buoy made out of steel. The main difference from WEPA is that the PTO is located inside the foundation instead of inside the buoy. Furthermore, the PTO is composed of a linear generator, while for WEPA the translational motion is transformed into rotational motion via the grooved drum. The reason behind this design choice is to simplify maintenance (maintenance operations can be performed by approaching the buoy with a boat or towing the buoy in to a shipyard). In addition, rotational generators are easier to find on the market and less expensive than linear generators.

Worth mentioning is also Wavebob, which uses a submerged volume rather than a damping plate as reference. However, the company closed in 2013 due to financial problems [18].

Fred Olsen's Lifesaver uses the heave motion (translation), and in addition, the pitch and roll motions (rotation), as it consists of a floating buoy with circular shape that has three mooring lines secured to the seabed. Each mooring line is connected to a PTO to harvest energy [19]. Compared to WEPA, the Lifesaver has two more PTOs, three in total, which may increase the productivity, but also the costs. Furthermore, the mooring system is more complex than the one designed for WEPA, as it has six mooring lines compared to the four of WEPA.

Carnegie has developed several versions of submerged point absorbers, and CETO 6 is the latest device developed by the company. It exploits the orbital motion a few meters below the surface to drive the PTO system and generate electricity [20,21]. Being a submerged WEC, CETO 6 is intrinsically different from WEPA, however in the past, Carnegie has developed several versions of CETOs with the purpose of water desalination. The difference from WEPA is related to the fact that the CETO uses directly pressurized water instead of electricity to power the desalination unit.

The device developed by Aquaharmonics consists of a floating buoy connected to the seabed thanks to a mooring line [22]. The PTO is connected to a sheave that the mooring line is wrapped around. The energy production is optimized thanks to PTO stiffness and damping tuning [23]. The Aquaharmonics working principle is similar to WEPA; however, the WEPA concept is based on the dual production of energy and freshwater. Additionally, the hull shape and size is different.

1.4. Comparison with Existing Optimization Studies

Several studies have address the WEC optimization processes [24], but the main difference is that the present study is based on a real case study. It investigates the key parameters required to complete design and prototype construction. Many optimization studies focused on floating single-body point absorbers do not include a techno–economic analysis [25,26]. The work presented by [27,28] provide useful hints about the optimization of the shape of a wave-energy collector using genetic algorithms, however, they do not include PTO sizing, and the cost functions are simplified and do not include components costs. The study is mainly focused on the shape optimization rather on the whole WEC optimization. The interesting study presented by [29,30] shows an optimization process based on an evolutionary algorithm for different WECs, however, the PTO extra cost in the parametric analysis is not included, just the buoy cost. This provide useful information for sizing but not for the optimal configuration selection. According to [31,32], it is important to substitute cost proxies based on the device's submerged volume with cost proxies based on actual submerged surface area. However, it is not considered the cost of the internal equipment. Furthermore, their analysis is developed in the frequency domain, while the one presented in this study is developed in the time domain. None of the studies reviewed

include layout constraints, due to the volume of the internal equipment to locate inside the hull. This was found to be one of the major challenge in our work, as highlighted in Section 3.2.2.

Finally, the remainder of the paper is organized as follows. Section 2 describes the simulation tool, the mathematical model used, and the model verification. The main results of the modelling and techno–economic analysis are summarized in Section 3. Finally, the conclusions are drawn in Section 4.

2. Materials and Methods

2.1. The Simulation Tool

The WEPA design and optimization process is based on a simulation tool, developed jointly by Wave for Energy Srl and Politecnico di Torino. As summarized in Figure 3, the model requires as input data the hydrodynamic properties of the body (further described in Section 2.2.2) and the irregular wave profile obtained from the site-specific statistical data, such as significant wave height and period (further described in Section 2.2.1). A further improvement to the model would be represented by the use of a genetic optimization [33].

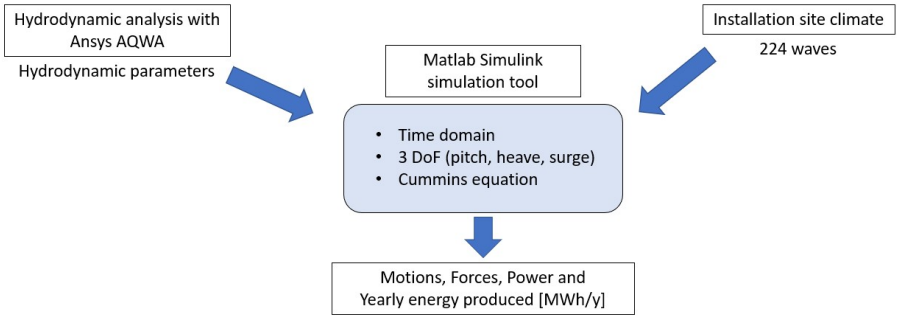

Figure 3. Simulation tool working principle.

The simulation tool uses time-domain mathematical models based on the Cummins equation. It uses Matlab-Simulink environment to solve the ordinary differential equations. The following equation is used to simulate the buoy motion due to the external forces acting on it [34–36].

$$(M + A_\infty) \cdot \ddot{x}(t) + F_r = F_e + F_{visc} + F_h + F_p + F_{PTO} \quad (1)$$

where:

M mass/inertia matrix
A_∞ added mass matrix at infinite frequency
F_r force due to radiation phenomenon
F_e wave excitation forces acting on the dynamic system
F_{visc} force due to viscous phenomenon
F_h hydrostatic buoyancy force
F_p mooring system pretension force
F_{PTO} total PTO force.

Furthermore, the F_{PTO} term, which represents the equivalent force generated by the PTO, can be written as:

$$F_{PTO} = F_{pto,k} + F_{pto,c} \quad (2)$$

where:

$F_{pto,k}$ restoring force due to the stiffness
$F_{pto,c}$ PTO damping force.

The PTO stiffness and damping can be tuned to maximize energy production. In fact, for each wave simulated, different damping coefficients are tested. Subsequently, during the optimization phase, the damping coefficient that corresponds to better energy yield is

selected. The influence of the PTO stiffness is also studied thanks to a sensitivity analysis. The current numerical model is based on three degrees of freedom. Heave, surge and pitch are enough to simulate an oscillating device in the sea and provide a realistic view of the point absorber motions. The outputs of the model are the motions and forces at every time step for the entire duration of the simulation. A simulation is performed for each wave occurring at the installation site to cover all the sea states the WEC is statistically exposed to. The power can be calculated according to Equation (3) from the tether velocity, the unwinding drum velocity, and the PTO damping, which is a control parameter.

$$P = \beta \cdot v^2 \tag{3}$$

With:

P gross power [W]
β PTO damping coefficient [kg/s]
v tether velocity [m/s].

Torque and power are saturated using the specific PTO data taken from the commercial products selected for the analysis. Computing the average power extracted for a specific wave and multiplying it by its occurrence, in hours, provide the mean energy extracted from that specific sea state. Summing up the contributions of each wave occurring at the installation site in terms of energy produced, the yearly energy production of the device can be computed.

2.2. Input Data

As described in Figure 3, the main input data needed to run the model are the environmental conditions of the installation site and the hydrodynamic parameters of the floater as well as the modelling parameters.

2.2.1. Environmental Input Data

The environmental input data used for this analysis are limited to wave statistical data and the water depth of the installation site. Additionally, current and wind may affect the hydrodynamic behaviour of the buoy, however, they are neglected in this analysis as the impact on productivity is negligible. The combination of significant wave height and peak period are used to generate irregular wave forces for the time-domain analysis. The wave forces are generated using JONSWAP spectrum with peak enhancement factor γ of 3.3. The water depth considered is 25 m. The seawater density is 1025 kg/m^3. The specific wave input data used for this analysis are taken from [37] and presented in Figure 4.

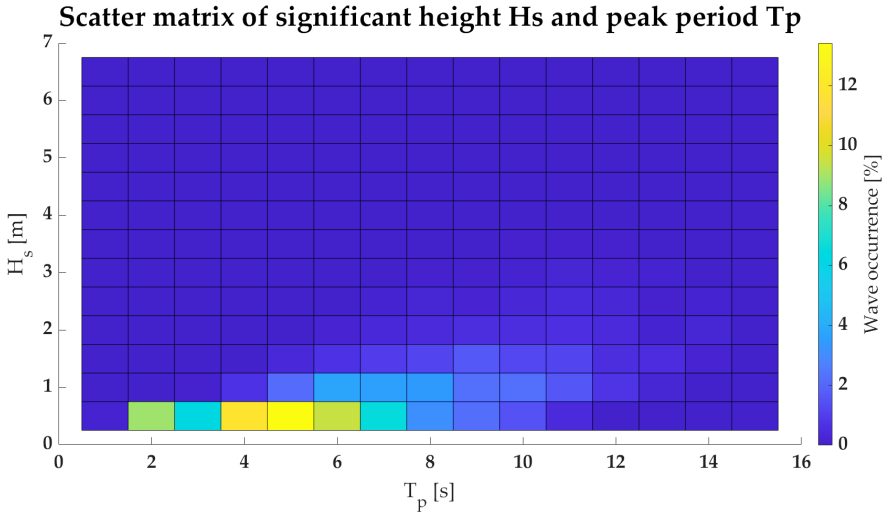

Figure 4. Scatter matrix of significant height, Hs [m], and peak period, Tp [s], for the case study. Based on data available from [37].

2.2.2. Hydrodynamic Input Data

The calculation of the hydrodynamic parameters requires a Boundary Element Method (BEM) software. It uses a fine mesh-based spatial discretization of the wetted surface of the hull to solve the linear potential flow problem [38]. The Hydrodynamic Diffraction package of Ansys AQWA is used as BEM solver in this study. The drag coefficients used in this analysis are reported in Table 1.

Table 1. Drag coefficients adapted from [39].

Cd_x,Cd_y	Cd_z	Cd_θ
0.7	1.28	0.22

2.2.3. Modelling Parameters

The dynamic simulations are run for 1200 s with a time step of 0.01 s. The Matlab-Simulink Ode45 solver is used to compute the ordinary differential equation.

2.3. Optimization

The main optimization parameter of WEPA is the PTO damping coefficient. For each sea state (combination of Tp and Hs), many simulations are run, changing the PTO damping coefficient. The PTO damping coefficient that corresponds to the higher yearly energy production is selected during the optimization process, which is performed subsequently to the simulation phase. As described in Section 2.1, the simulation tool saturates PTO torque and power, and on the contrary, the PTO velocity is set free. During the postprocessing optimization phase, the simulations with PTO velocity higher than allowable (from generator data sheet) are discarded. Therefore, the energy yield for each wave is computed considering the PTO damping coefficient that maximizes energy production but that does not exceed maximum velocity and torque. This is to safeguard the generator integrity and provide as output a reliable energy yield for each sea state.

2.4. Model Verification

The simulation tool previously described is verified with a commercial software to evaluate its accuracy. The commercial software used is Orcaflex 11.0 b developed by Orcina. The verification is performed both in regular and irregular waves. The same wave profile used for the Matlab-Simulink model is imported into the Orcaflex model to ensure that the same wave elevation is recorded. The results are analyzed in terms of relative error of the Matlab-Simulink model respect to the Orcaflex model. The main parameter used in the verification is the tether velocity as the energy production is estimated from the velocity, as presented in Equation (3).

2.4.1. Regular Wave

The model comparison proved that the relative error in the regular wave is limited, and thus, the Matlab-Simulink model is validated for energy production estimation. The analysis is based on seven regular waves with constant height and period from 4 to 10 s with step 1 s. For each wave, Root Mean Square (RMS) and maximum values are computed. As shown in Figure 5, the relative errors of the RMS values are always lower than 6%. The maximum values have higher relative errors than RMS, and this can be explained by the fact that Orcaflex is able to better follow the peaks, however, rare peaks do not have significant influence on average energy production. The model is therefore considered suitable for the purpose of energy yield estimation, however, it is not suitable for WEC sizing, where the peak loads are more important for hull and mooring system sizing.

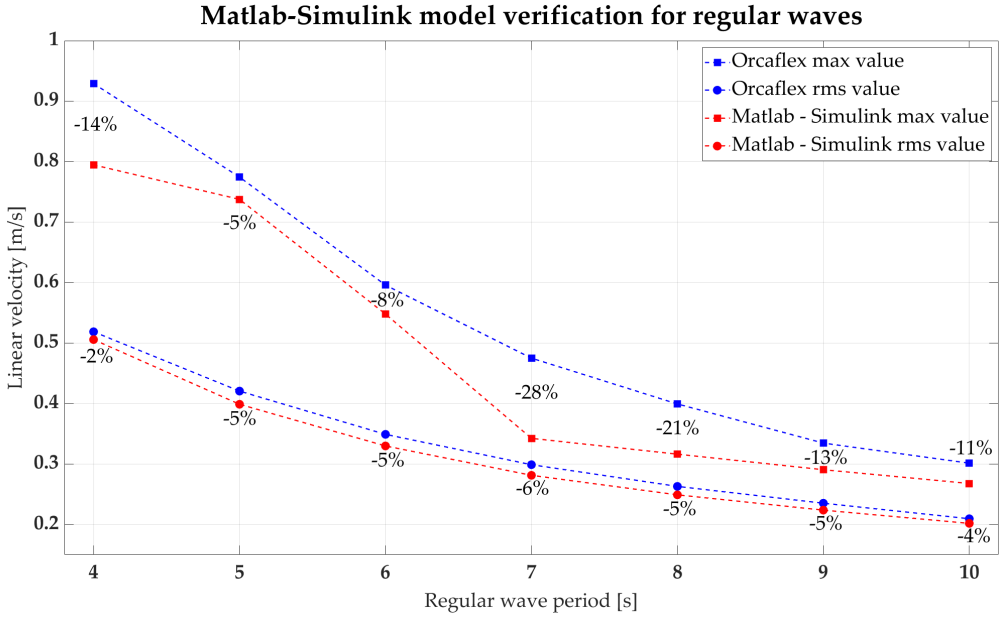

Figure 5. Regular wave comparison between Orcaflex and the Matlab-Simulink tool.

2.4.2. Irregular Wave

The analysis carried out on irregular waves shows that the model's fidelity is not as high as for regular waves. The number of waves tested is three, chosen among the most productive ones. As shown Figure 6, the maximum relative error for the RMS values is 13%. In all cases, the velocities obtained with the Matlab-Simulink model are lower than Orcaflex. The relative errors for the maximum values recorded during each simulation are higher than RMS values, and the highest is 35%.

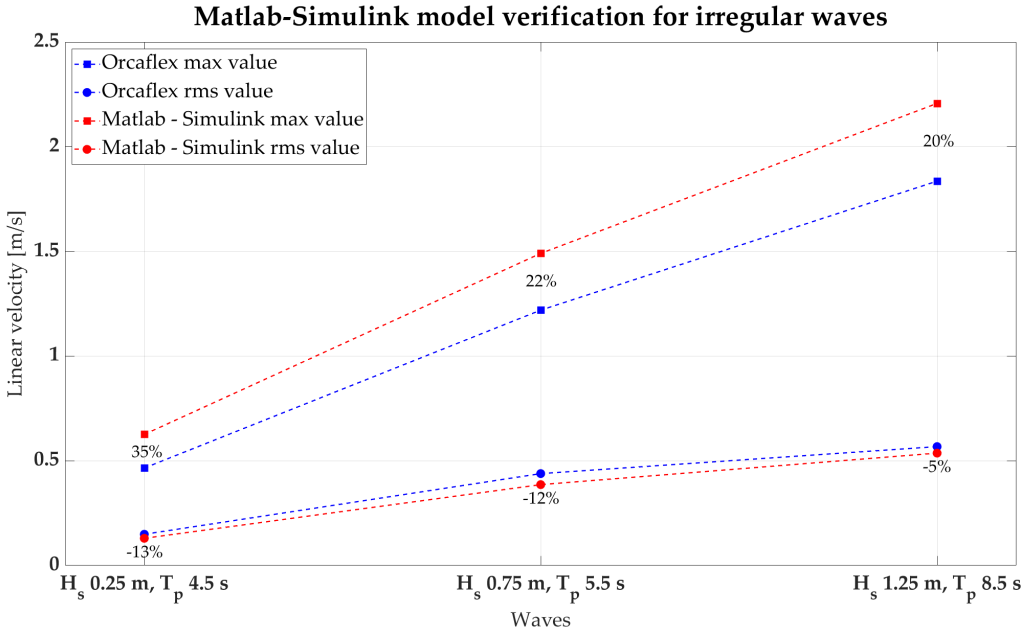

Figure 6. Irregular wave comparison between Orcaflex and the Matlab-Simulink tool.

Overall, the model can be considered reliable for an initial optimization process, as the short computational time allows for the screening of many configurations. To obtain information for the WEC sizing, such as mooring lines loads, Orcaflex software or others shall be used, as the Matlab-Simulink tool does not correctly identify the peaks [40].

3. Results

Two principal analyses are carried out in this study to optimize the WEC for the given site: the first involves an extensive parametric analysis of the main sizing parameters, while the second focuses on techno–economic optimization. The first investigation includes a sensitivity analysis on the generator sizing parameters, notably, rated speed, rated torque and gear ratio. The second part of the work focuses on the buoy characteristics: buoy size, height, mass and draft. Then, the control parameters are studied: PTO stiffness and damping. Finally, some considerations on the mooring stiffness are presented. All the analyses carried out in this study are summarized in the following subsections. To compare the performance of each configuration, the normalized gross energy production is presented, and it is computed as the percentage of gross energy production with respect to the highest value of the sensitivity analysis. All the simulations are performed with a cylindrical-shaped geometry. The mass is estimated considering the buoy volume and half of the water density. The pretension, and thus the equivalent stiffness, is computed to keep the draft as 63% of overall hull height. The main parameters are reported for each set of simulations.

3.1. Parametric Analysis

3.1.1. Generator Nominal Speed and Torque Sensitivity Analysis

This sensitivity analysis aims to understand the variation in terms of performance when changing generator sizing parameters to optimize WEPA for the given site. The two main generator sizing parameters are nominal speed and nominal torque. Table 2 reports the main features of the generators included in the analysis. The data reported in Table 2 are adapted from a commercial data sheet [41] to be more realistic in the PTO identification and facilitate the subsequent prototype design. The generator used, if not differently stated, is the 1FW3204H.

Table 2. Main features of generators included in the analysis adapted from [41].

Generator ID	Rated Speed [rpm]	Rated Torque [Nm]	Max Torque [Nm]	Rated Power [kW]
1FW3203E	150	750	1390	11.8
1FW3203H	300	750	1390	23.6
1FW3203L	500	750	1390	39.3
1FW3204E	150	1000	1850	15.7
1FW3204H	300	1000	1850	31.4
1FW3204L	500	1000	1850	52.3
1FW3206E	150	1500	2775	23.6
1FW3206H	300	1500	2775	47.1
1FW3206L	500	1400	2775	73.3
1FW3281E	150	2500	4050	39.0
1FW3283E	150	3500	5700	55.0
1FW3283G	250	3450	5700	90.0

As shown in Figure 7, the gross productivity is strongly influenced by the PTO-rated torque. On the contrary, the PTO-rated speed does not significantly affect the productivity. The generators “1FW3203H”, “1FW3204H” and “1FW3206H” have all the same rated speed of 300 rpm, while rated torque is of 750 Nm, 1000 Nm and 1500 Nm respectively. The results show that the energy yield grows with the PTO torque for these configurations. The same is valid for the generators “1FW3206E”, “1FW3281E” and “1FW3283E”. On the other hand, the generators with the same rated torque but different rated speed show similar energy yields. This is the case of the PTOs: “1FW3206E” and “1FW3206H”, which have rated torque of 1500 Nm; as well as the PTOs: “1FW3283E” and “1FW3283G”, which have rated torque of 5700 Nm. This trend is because the optimizer identifies as optimal high damping coefficients, which keeps the speed low but requires high torque. During regular

operation, the maximum speed is rarely reached; therefore, no power is lost due to velocity saturation. On the other hand, higher values of nominal and maximum torques allow the motor to extract more power without incurring torque saturation, which must be avoided to preserve the motor's integrity.

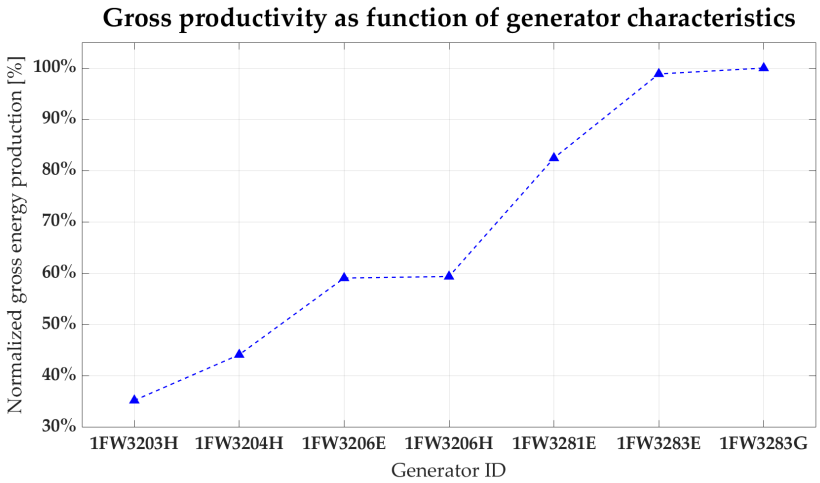

Figure 7. Gross productivity as function of generator characteristics.

In order to increase the energy production, torque saturation shall be reduced; therefore, generators with higher available torque are required. To increase available torque, scaling up of the generator is a solution; however, they grow proportionally in size and weight as they increase maximum torque. Alternatively, an additional component, such as a gearbox, can be inserted between the grooved drum and the generator. The gearbox is able to modify the ratio between torque and speed according to the size of the internal gears. The parameter used is the gear ratio, which is defined as the ratio of the angular speed of the initial member to that of the driven member. Thanks to the aforementioned considerations, an additional analysis is performed.

3.1.2. Gear Ratio Sensitivity Analysis

The objective of this sensitivity analysis is to understand the variation in terms of performance when inserting a gearbox in the model and changing the gear ratio to optimize WEPA for the given site. The gear ratios considered are from 2 to 5 with a step of 1. The analysis is performed with generators: "1FW3204L" and "1FW3206L", as they have very high nominal speeds. As shown in Table 2, they have a rated speed of 500 rpm.

The general trend highlighted with the direct-drive configuration (Figure 7) remains unchanged in this sensitivity analysis: generators with higher nominal torques paired with the gearbox with higher ratio are the most productive. As can be seen from Figure 8 the gear ratio that maximizes the energy production is a function of the generator nominal torque. The productivity starts to drops for high gear ratios, when the velocities are too high and the speed saturation is reached.

3.1.3. Hull Size Sensitivity Analysis

This sensitivity analysis aims to understand the variation in terms of performance when changing the hull size to optimize WEPA for the given site. The main features of the six configurations analyzed are reported in Table 3. As shown in Table 3, the hull dimensions are increased proportionally.

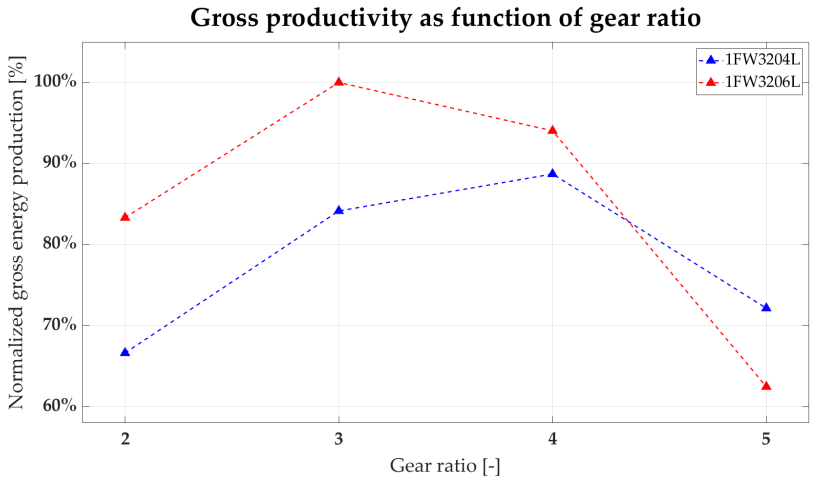

Figure 8. Gross productivity as function of gear ratio.

Table 3. Configuration parameters of hull size sensitivity analysis.

Hull	1.2 × 1.2	1.3 × 1.3	1.4 × 1.4	1.5 × 1.5	1.7 × 1.7	1.8 × 1.8
Height [m]	1.2	1.3	1.4	1.5	1.7	1.8
Radius [m]	1.2	1.3	1.4	1.5	1.7	1.8
Mass [kg]	2782	3537	4418	5434	7910	9390
Volume [m^3]	5.43	6.90	8.62	10.60	15.43	18.32
Draft [m]	0.76	0.82	0.88	0.94	1.07	1.13
Ixx [kgm^2]	1335	1993	2886	4075	7620	10,141
Iyy [kgm^2]	1335	1993	2886	4075	7620	10,141
Izz [kgm^2]	2003	2989	4330	6113	11,430	15,212
COG * [m]	−0.16	−0.17	−0.18	−0.19	−0.22	−0.23

* COG location is expressed as the distance from the water level.

From Figure 9, the trend is clear: in the given wave climate, the smaller hulls perform better in energy production. This behaviour could be counterintuitive at a first superficial analysis. However, this is strictly related to the resonance frequency of the device and the incoming waves. As stated by [24,42], for heaving vertical cylinders, smaller devices perform better in high wave frequency as they tend to have higher natural frequency and vice versa. As shown in Figure 4, most waves have a peak period among 2 and 7 s; these high-frequency waves better match with small-sized hulls. The main constraint to building small hulls is the lack of internal space to locate all the required equipment, so a sensitivity analysis on the hull height is performed.

3.1.4. Hull Height Sensitivity Analysis

The objective of this sensitivity analysis is to understand the variation in terms of performance when changing the hull height to optimize WEPA for the given site. The main features of the configurations analyzed are reported in Table 4. The hull height varied from 1 m to 1.6 m with step 0.2 m, for a total of four configurations.

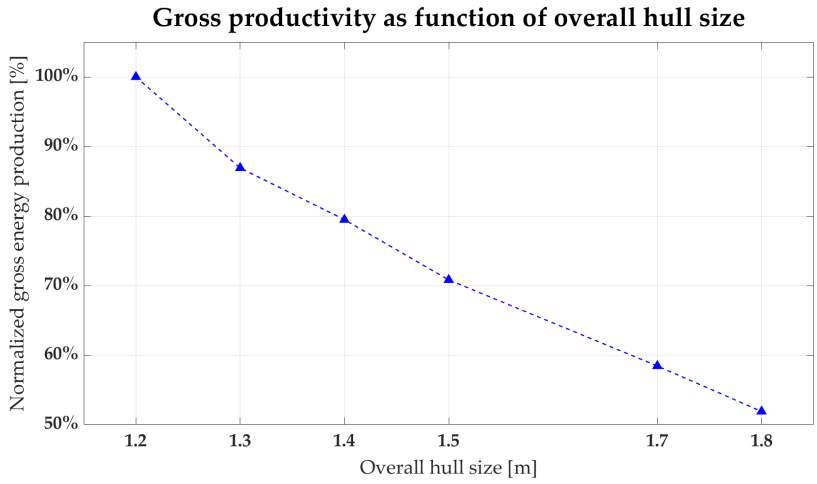

Figure 9. Gross productivity as function of overall hull size.

Table 4. Configuration parameters of hull height sensitivity analysis.

Hull	1.2 × 1.0	1.2 × 1.2	1.2 × 1.4	1.2 × 1.6
Height [m]	1	1.2	1.4	1.6
Mass [kg]	2199	2782	3365	3949
Volume [m^3]	4.52	5.43	6.33	7.24
Draft [m]	0.63	0.76	0.88	1.01
Ixx [kgm^2]	975	1335	1761	2264
Iyy [kgm^2]	975	1335	1761	2264
Izz [kgm^2]	1583	2003	2423	2843
COG * [m]	−0.13	−0.16	−0.18	−0.21

* COG location is expressed as the distance from the water level.

As shown in Figure 10, the influence of hull height on gross productivity is limited. If the height is increased, the productivity increases. As the draft is calculated as a percentage of the overall height, the draft increases for larger heights, as shown in Table 4. The larger submerged volume and wetted surface increase the drag force, improving the ability of the buoy to follow the wave elevation profile. This information is helpful during the design phase, as a large number of components have to be integrated inside the hull. As a consequence, the internal volume can be enlarged, increasing the hull height without negatively impacting the performances.

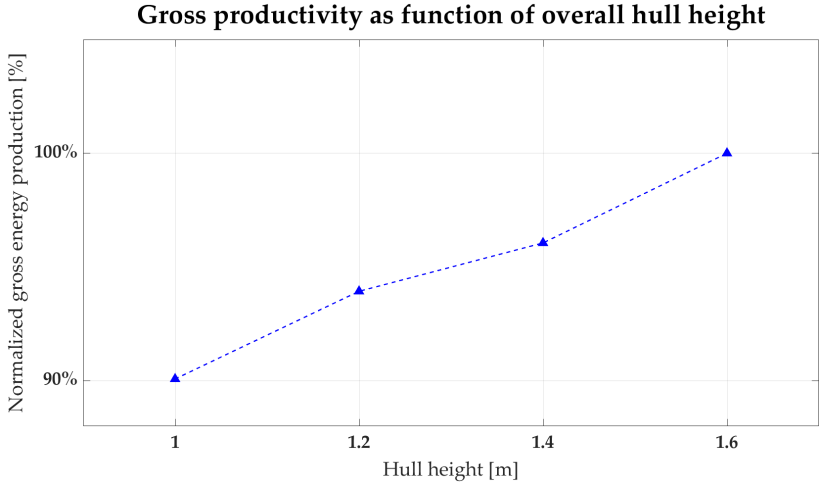

Figure 10. Gross productivity as function of overall hull height.

3.1.5. Hull Mass Sensitivity Analysis

This sensitivity analysis aims to understand the variation in terms of performance when changing the hull mass to optimize WEPA for the given site. The buoy mass was originally estimated as 50% displaced water weight. The study investigated the performance of a buoy with 30% and 60% displaced water weight. The draft is kept constant, while the mooring pretension is changed to adjust buoy equilibrium. The main features of the three configurations analyzed are reported in Table 5.

Table 5. Configuration parameters of hull mass sensitivity analysis.

Hull	1.3 × 1.3-Mass 30%	1.3 × 1.-Mass 50%	1.3 × 1.3-Mass 60%
Height [m]	1.3	1.3	1.3
Mass [kg]	2122	3537	4245
Volume [m^3]	6.90	6.90	6.90
Draft [m]	0.82	0.82	0.82
Ixx [kgm^2]	1196	1993	2391
Iyy [kgm^2]	1196	1993	2391
Izz [kgm^2]	1794	2989	3587
COG * [m]	−0.17	−0.17	−0.17

* COG location is expressed as the distance from the water level.

As shown in Figure 11, gross energy production variation due to the hull mass included among 2.1 t and 4.2 t is limited to 10%. The higher mass is related to higher productivity; this information is helpful during the design phase as it increases the ballast to reach stability of the buoy.

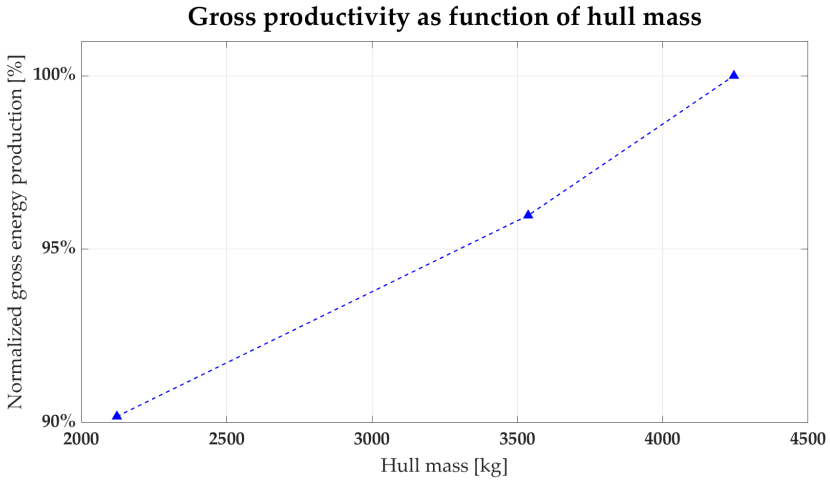

Figure 11. Gross productivity as function of hull mass.

3.1.6. Hull Draft Sensitivity Analysis

This sensitivity analysis aims to understand the variation in terms of performance when changing the hull draft to optimize WEPA for the given site. The study investigated the performance of a buoy with the draft equal to 70%, 75% and 80% of overall height. The tether pretension is kept constant, while the mass is changed to adjust buoy equilibrium. The main features of the three configurations analyzed are reported in Table 6.

Table 6. Configuration parameters of hull draft sensitivity analysis.

Hull	1.2 × 1.2-Draft 70%	1.2 × 1.2-Draft 75%	1.2 × 1.2-Draft 80%
Height [m]	1.2	1.2	1.2
Mass [kg]	3178	3456	3734
Volume [m^3]	5.43	5.43	5.43
Draft [m]	0.84	0.90	0.96
Ixx [kgm^2]	1525	1659	1792
Iyy [kgm^2]	1525	1659	1792
Izz [kgm^2]	2288	2488	2689
COG * [m]	−0.24	−0.30	−0.36

* COG location is expressed as the distance from the water level.

As shown in Figure 12, the draft sensitivity analysis showed limited correlations with productivity. This was also expected from Figure 10, as increasing the overall height increases the draft as well.

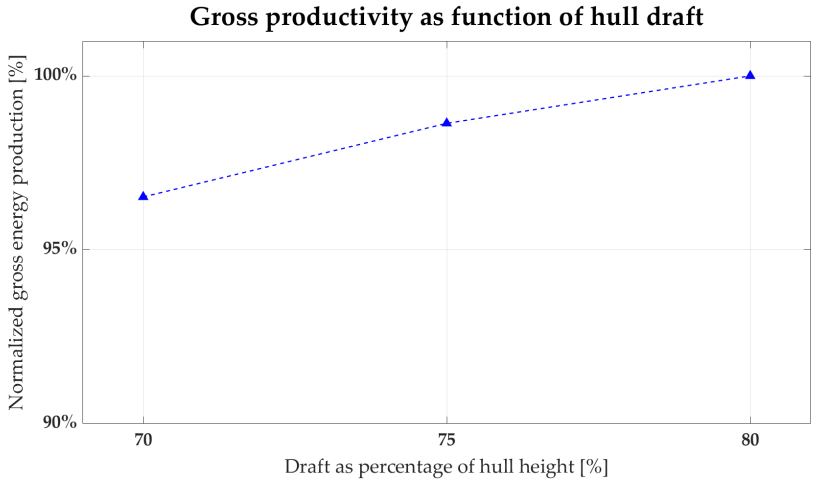

Figure 12. Gross productivity as function of hull draft.

3.1.7. Control Parameters

The PTO-related variables which influence the power extraction of the device are the PTO damping coefficient and the PTO stiffness, as shown in Equation (2). The former, multiplied by the shaft's rotating speed, provides the torque generated by the hull heave motion and thus the extracted power. The latter, multiplied by the production tether elongation, provides the rewinding force that is required to keep the production tether in tension. The optimal value of PTO damping for each sea state, the one that optimizes the power extraction, varies greatly with the height and period of incoming waves, with lower values preferred on smaller waves and higher ones favored on higher waves, as can be seen in Figure 13. Thanks to the adopted control strategy, a specific PTO damping coefficient will be defined for each sea state. The optimal value for PTO stiffness is close to zero. However, it is necessary to guarantee that the production tether remains in tension at every given moment. Therefore, a positive PTO stiffness shall be provided. The PTO stiffness can be provided by the PTO working in motor mode or by an actual spring mounted on the shaft.

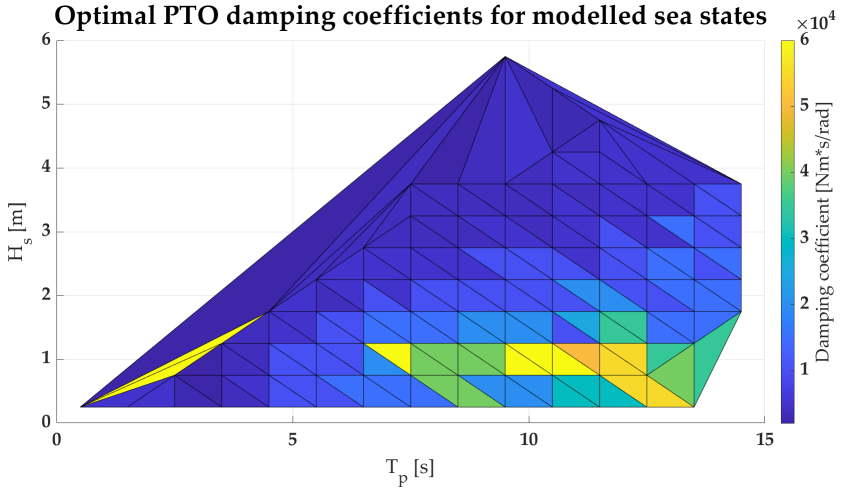

Figure 13. Optimal PTO damping coefficients for the modelled sea states.

3.1.8. Mooring Stiffness

The mooring system included in the simulation tool comprises a single line connecting the sea bottom to the hull as the DoF considered in the analysis are two translations (heave and surge) and one rotation (pitch). The restoring forces due to the mooring line stiffness are included via a constant stiffness parameter. The mooring line stiffness coefficient multiplies the mooring cable elongation, giving as a result the restoring force applied by the mooring lines on the hull. The simulations clearly show how the mooring line stiffness should be as low as possible. This is because the higher the stiffness, the higher the influence of the mooring lines on the hull motions, reducing its velocity and negatively impacting productivity.

3.2. Techno–Economic Analysis

The optimization strategy aims at finding the best device for the installation site, where the "best" can be different according to different criteria (the lowest cost of energy, the highest productivity depending on investment thresholds, highest site-insensitive productivity, for example). The performance index used in this analysis is measured in kEUR/MWh (EUR over megawatt-hour), and is the ratio between the total capital cost over the total energy produced per year:

$$Performance\ Index\ (PI) = \frac{Device\ Cost\ [k€]}{Net\ Productivity\ [\frac{MWh}{year}]} \tag{4}$$

While the energy production is straightforward to compute thanks to the simulation tool, quantifying total costs requires additional input data and a detailed feasibility study.

3.2.1. Cost Analysis

Four sources of variable costs are considered in this study: the generator and its drive, the mechanical internal components, the hull, and the mooring system. The rest of the costs are considered equal for all the configurations and thus excluded from the analysis.

Generator and Drive Costs

To approximate generators and drives costs, Equations (5) and (6) are used, respectively. They are in-house interpolations based upon the authors' market surveys and quotations.

$$Generator\ cost\ [k€] = 1.0582t^3 - 48.431t^2 + 899.26t - 4780.5 \tag{5}$$

where t is the generator rated torque in [Nm].

$$Drive\ cost\ [k€] = 2.6615p^3 - 25.742p^2 + 90.118p - 92.244 \quad (6)$$

where p is the generator rated power in [kW].

Hull Cost Estimation

The hull cost is estimated computing the overall weight thanks to an equivalent thickness of 18 mm. The unitary cost is fixed to 12 EUR /kg. The cost is estimated as shown in Equation (7).

$$C_h\ [k€] = [2\pi R^2 + 2\pi RH + 2(1 + 0.6)H]T_u\rho_s C_u \quad (7)$$

with:

C_h hull cost [kEUR]
R buoy radius [m]
H buoy height [m]
C_u unitary cost [kEUR/kg]
T_u equivalent thickness [m]
ρ_s steel density [kg/m^3].

Mooring Cost Estimation

The mooring system costs are analyzed in detail for a single configuration; further, the total cost is scaled according to the buoy submerged volume. The submerged volume is directly proportional to mooring loads; thus, the mooring system cost is scaled according to design tension.

Mechanical Internal Components Cost Estimation

The internal mechanical components costs are analyzed in detail for a single configuration; further, the total cost is scaled according to max torque.

3.2.2. Feasibility Study

Once the cost analysis is completed, it is possible to score the different configurations according to the PI, and thus, select the best devices for a more accurate feasibility study. The feasibility study included considerations on the electrical system, the mechanical components and layout. The electrical system is studied in more detail and all the equipment to be installed on-board is identified. A preliminary mechanical drawing of the main components is accomplished, and the general layout of the device is built. The main constraint is found to be the layout, therefore a specific analysis is carried out to eliminate the configurations that are considered unfeasible due to dimensional constraints. The main problem is due to the length of the generator, the drum and the joints. Figure 14 shows the feasibility analysis for a configuration with an external radius of 1.3 m.

It is worth mentioning that from the feasibility study and cost analysis, the gearbox configuration, which initially appeared highly interesting, manifested two essential drawbacks. From an engineering standpoint, the encumbrance of both the gearbox and the motor is greater than a larger PTO only, therefore, larger hulls are required. From the economic analysis, the cost of the gearbox itself is high enough to nullify the advantage of using a smaller and less expensive generator.

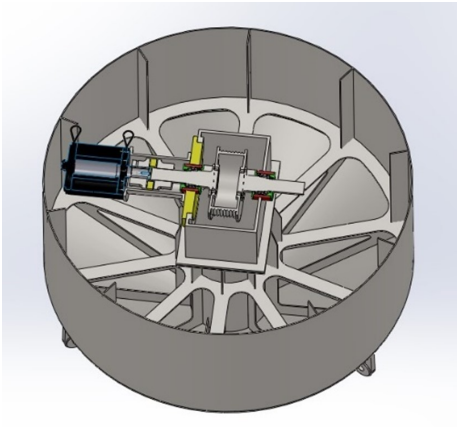

Figure 14. PTO and hull feasibility analysis.

3.2.3. Final Selection

As a result of the feasibility analysis, a large number of configurations are discarded due to unfeasibility or excessive costs. Figure 15 presents the results of the techno–economic analysis. The Figure presents the normalized device cost and gross energy production of the different configurations analyzed, the normalized device cost is computed dividing the cost of all the devices by the highest. The bottom-right corner area of the Figure is where the most interesting configurations are located. Starting from the configurations with lower PI, a feasibility study is carried out and the grey area is drawn. The grey area in Figure 15 identifies the configurations that, after the feasibility, were not feasible. Finally, two optimal configurations are selected, one with higher productivity and higher investment costs and one with lower productivity but lower costs.

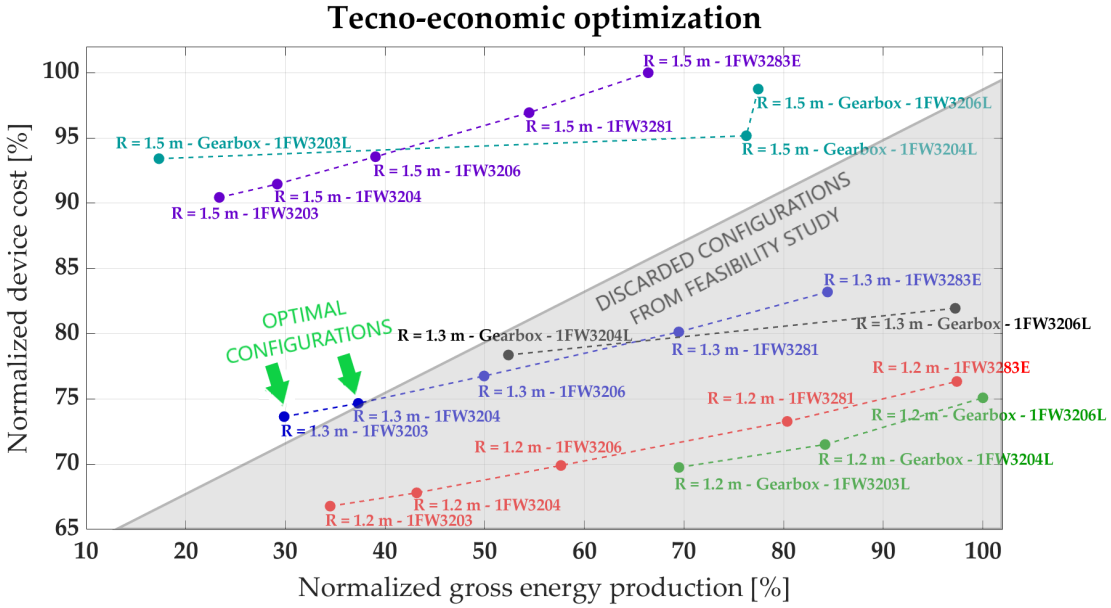

Figure 15. Normalized device cost and gross energy production of different configurations analyzed (the grey area is considered unfeasible).

4. Conclusions

This paper presents the Water Energy Point Absorber (WEPA); its concept is compared to other existing WECs, highlighting the differences and the improvements from the state of the art. The simulation tool developed to perform the optimization study is presented and the mathematical models and the assumptions on which it is based on. The input data used for the analysis are reported, such as the wave scatter matrix, the hydrodynamic parameters and the modelling settings. The optimization principle is explained and the

model verification is introduced. The model verification is performed with regular and irregular waves thanks to the commercial software Orcaflex.

Several parametric analyses are performed to reach an optimal final design in terms of performances and costs for the specific installation site. Among the results of the analysis performed, it shall be mentioned that the PTO-rated torque is more impactful than the rated speed in terms of gross energy production. In particular, the higher the rated torque, the higher the productivity. A gearbox can be added to increase the available torque and the optimal gear ratio can be computed from the simulations. However, from the cost analysis, it is shown that the additional cost of the gearbox does not compensate the additional energy produced. The most important highlight of the study is that for the specific wave climate the smaller hulls are performing better than the bigger ones. This is due to the natural frequency of the hulls that is closer to the one of the incoming waves. A sensitivity analysis is also run for hull height, hull mass and hull draft, showing that their influence on productivity is limited. Finally, a comprehensive techno–economic analysis is presented, demonstrating that the optimal configuration can be identified only after a detailed feasibility study and rigorous cost analysis.

Author Contributions: Conceptualization, M.R.; methodology, M.R. and P.D.; software, M.R. and V.M.; validation, M.R. and V.O.; formal analysis, M.R. and P.D.; investigation, M.R.; resources, M.R., A.G., G.M. and G.B.; data curation, M.R.; writing-original draft preparation, M.R.; writing—review and editing, M.R., G.G. and V.M.; visualization, V.M.; supervision, V.O., G.M., G.B. and G.G.; project administration, M.R. and P.D.; funding acquisition, M.R., G.M. and A.G. All authors have read and agreed to the published version of the manuscript.

Funding: This research was partially funded thanks to the project "WAVES4WATER", funding line: "PROMOZIONE DI NUOVI MERCATI PER L'INNOVAZIONE NELLA PA". POR FESR SARDEGNA 2014/2020. ASSE PRIORITARIO I. RICERCA SCIENTIFICA, SVILUPPO TECNOLOGICO E INNOVAZIONE AZIONE 1.3.1.

Institutional Review Board Statement: Not applicable.

Informed Consent Statement: Not applicable.

Data Availability Statement: Data available on request due to restrictions eg privacy or ethical. The data presented in this study are available on request from the corresponding author. The data are not publicly available due to confidentiality agreement with partners.

Acknowledgments: The authors gratefully acknowledge the General Director Mariano Mariani of Parco Naturale Regionale di Porto Conte e Area Marina Protetta Capo Caccia—Isola Piana, as well as the team composed by Pasquale Sinis, David Pala and Alberto Ruiu.

Conflicts of Interest: The authors declare no conflicts of interest.

Abbreviations

The following abbreviations are used in this manuscript:

BEM	Boundary Element Method
COG	Center of Gravity
DoF	Degree of Freedom
EUR	Euro
GHG	Green House Gasses
Hs	Significant Height
PI	Performance Index
PTO	Power Take Off
WEC	Wave Energy Converter
WEPA	Water Energy Point Absorber
RMS	Root Mean Square
TLA	Three
LD	Linear
Tp	Peak Period

References

1. Falcão, A.F.O. Wave energy utilization: A review of the technologies. *Renew. Sustain. Energy Rev.* **2010**, *14*, 899–918. [CrossRef]
2. Ilyas, A.; Kashif, S.A.; Saqib, M.A.; Asad, M.M. Wave electrical energy systems: Implementation, challenges and environmental issues. *Renew. Sustain. Energy Rev.* **2014**, *40*, 260–268. [CrossRef]
3. Guo, B.; Ringwood, J.V. A review of wave energy technology from a research and commercial perspective. *IET Renew. Power Gener.* **2021**, *15*, 3065–3090 [CrossRef]
4. Shadman, M.; Estefen, S.F.; Rodriguez, C.A.; Nogueira, I.C. A geometrical optimization method applied to a heaving point absorber wave energy converter. *Renew. Energy* **2018**, *115*, 533–546. [CrossRef]
5. Aderinto, T.; Li, H. Ocean Wave energy converters: Status and challenges. *Energies* **2018**, *11*, 1250. [CrossRef]
6. Faraggiana, E.; Chapman, J.C.; Williams, A.J.; Masters, I. Genetic based optimisation of the design parameters for an array-on-device orbital motion wave energy converter. *Oceans Eng.* **2020**, *218*, 108251. [CrossRef]
7. Bracco, G.; Giorcelli, E.; Mattiazzo, G.; Pastorelli, M.; Taylor, J. ISWEC: design of a prototype model with gyroscope. In Proceedings of the 2009 International Conference on Clean Electrical Power, Capri, Italy, 9–11 June 2009; pp. 57–63. [CrossRef]
8. Mattiazzo, G. State of the Art and Perspectives of Wave Energy in the Mediterranean Sea: Backstage of ISWEC. *Front. Energy Res.* **2019**, *7*, 114. [CrossRef]
9. Liu, Z.; Zhang, R.; Xiao, H.; Wang, X. Survey of the mechanisms of power take-off (PTO) devices of wave energy converters. *Acta Mech. Sin./Lixue Xuebao* **2020**, *36*, 644–658. [CrossRef]
10. Cretel, J.A.; Lightbody, G.; Thomas, G.P.; Lewis, A.W. Maximisation of energy capture by a wave-energy point absorber using model predictive control. *IFAC Proc. Vol.* **2011**, *44*, 3714–3721. [CrossRef]
11. Bizzozero, F.; Bozzi, S.; Gruosso, G.; Passoni, G.; Giassi, M. Spatial interactions among oscillating wave energy converters: Electricity production and power quality issues. In Proceedings of the IECON 2016-42nd Annual Conference of the IEEE Industrial Electronics Society, Florence, Italy, 23–26 October 2016; pp. 4235–4240. [CrossRef]
12. Amponsah, N.Y.; Troldborg, M.; Kington, B.; Aalders, I.; Hough, R.L. Greenhouse gas emissions from renewable energy sources: A review of lifecycle considerations. *Renew. Sustain. Energy Rev.* **2014**, *39*, 461–475. [CrossRef]
13. Pecher, A.; Kofoed, J.P. *Handbook of Ocean Wave Energy*; Springer: Berlin/Heidelberg, Germany, 2017; p. E1. [CrossRef]
14. Wave Devices: EMEC: European Marine Energy Centre. Available online: https://www.emec.org.uk/marine-energy/wave-devices/ (accessed on 26 October 2021) .
15. Drew, B.; Plummer, A.R.; Sahinkaya, M.N. A review of wave energy converter technology. *Proc. Inst. Mech. Eng. Part A J. Power Energy* **2009**, *223*, 887–902. [CrossRef]
16. Wave Developers: EMEC: European Marine Energy Centre. Available online: https://www.emec.org.uk/marine-energy/wave-developers/ (accessed on 26 October 2021).
17. SEABASED. Available online: https://seabased.com/ (accessed on 27 October 2021) .
18. Downing, L. Wavebob Shuts Down after Failing to Raise Funds, Find Partner. 2013. Available online: https://www.bloomberg.com/news/articles/2013-04-03/wavebob-shuts-down-after-failing-to-raise-funds-find-partner (accessed on 27 October 2021).
19. Cross, P.; Rajagopalan, K.; Druetzler, A.; Argyros, A.; Joslin, J.; Stewart, A. Recent Developments at the U.S. Navy Wave Energy Test Site. In Proceedings of the 13th European Wave and Tidal Energy Conference, Napoli, Italy, 1–6 September 2019; pp. 1–9.
20. CETO Technology-Carnegie. Available online: https://www.carnegiece.com/ceto-technology/ (accessed on 2 November 2021).
21. Sergiienko, N.Y. Three-Tether Wave Energy Converter: Hydrodynamic Modelling, Performance Assessment and Control. Ph. D. Thesis, School of Mechanical Engineering The University of Adelaide Adelaide, Adelaide, Australia, 2018.
22. Saeidtehrani, S.; Lomonaco, P.; Hagmuller, A.; Levites-ginsburg, M.; Lom, P.; Hagm, A.; Levites-ginsburg, M. Application of a simulation model for a heave type wave energy converter. In Proceedings of the 12th European Wave and Tidal Energy Conference, Cork, Ireland, 27 August–1 September 2017; pp. 948-1–948-8.
23. Ginsburg, M.; Hagmüller, A. Control Co-Design of the AquaHarmonics Wave Energy Device. Available online: https://arpa-e.energy.gov/sites/default/files/5.%20Hagmuller_Aquaharmonics_Presentation.pdf (accessed on 10 January 2022).
24. Garcia-Teruel, A.; Forehand, D.I. A review of geometry optimisation of wave energy converters. *Renew. Sustain. Energy Rev.* **2021**, *139*, 110593. [CrossRef]
25. Gilloteaux, J.C.; Ringwood, J. Control-informed geometric optimisation of wave energy converters. *IFAC Proc. Vol.* **2010**, *43*, 366–371. [CrossRef]
26. Babarit, A.; Clement, A.H. Shape optimisation of the SEAREV wave energy converter. In Proceedings of the World Renewable Energy Conference, Florence, Italy, 19–25 August 2006.
27. McCabe, A.P.; Aggidis, G.A.; Widden, M.B. Optimizing the shape of a surge-and-pitch wave energy collector using a genetic algorithm. *Renew. Energy* **2010**, *35*, 2767–2775. [CrossRef]
28. McCabe, A.P. Constrained optimization of the shape of a wave energy collector by genetic algorithm. *Renew. Energy* **2013**, *51*, 274–284. [CrossRef]
29. Blanco, M.; Moreno-Torres, P.; Lafoz, M.; Ramírez, D. Design Parameter Analysis of Point Absorber WEC via an Evolutionary-Algorithm-Based Dimensioning Tool. *Energies* **2015**, *8*, 11203–11233. [CrossRef]
30. Blanco, M.; Lafoz, M.; Ramirez, D.; Navarro, G.; Torres, J.; Garcia-Tabares, L. Dimensioning of point absorbers for wave energy conversion by means of differential evolutionary algorithms. *IEEE Trans. Sustain. Energy* **2019**, *10*, 1076–1085. [CrossRef]

31. Garcia-Teruel, A.; Jeffrey, H.; Forehand, D.I.M. Metrics for wave energy converter hull geometry optimisation. In Proceedings of the 13th European Wave and Tidal Energy Conference, Napoli, Italy, 1–6 September 2019; pp. 1–6.
32. Garcia-Teruel, A.; DuPont, B.; Forehand, D.I. Hull geometry optimisation of wave energy converters: On the choice of the objective functions and the optimisation formulation. *Appl. Energy* **2021**, *298*, 117153. [CrossRef]
33. Sirigu, S.A.; Foglietta, L.; Giorgi, G.; Bonfanti, M.; Cervelli, G.; Bracco, G.; Mattiazzo, G. Techno-Economic optimisation for a wave energy converter via genetic algorithm. *J. Mar. Sci. Eng.* **2020**, *8*, 482. [CrossRef]
34. Dafnakis, P. Mathematical Modeling, Control and Dynamic Analysis of Point Absorber Wave Energy Converter Technology. Ph.D. Thesis, Doctoral Program in Mechanical Enginering, Turin, Italy, 2022
35. Falnes, J. Ocean waves and oscillating systems. *Dev. Sedimentol.* **2002**, *52*, 11–28. [CrossRef]
36. Alves, A.; Sarmento, A. Hydrodynamic Optimization of the Active surface of a Heaving Point Absorber WEC. In Proceedings of the 8th European Wave and Tidal Energy Conference, Uppsala, Sweeden, 7–10 September 2009; pp. 610–617.
37. *Allegato 1 Capitolato Tecnico Procedura Aperta per L'acquisizione di Servizi di Ricerca e Sviluppo ex art. 158, Comma 1, del D.lgs.50/2016 e ss.mm. e ii. per lo "Sviluppo di Nuove Tecnologie al Fine di Migliorare il Sistema di Approvvigionamento Energetic*; Technical Report; Area Marina Protetta Parco di Porto Conte: Tramariglio, Italy, 2021.
38. Fontana, M.; Casalone, P.; Sirigu, S.A.; Giorgi, G.; Bracco, G.; Mattiazzo, G. Viscous damping identification for a wave energy converter using CFD-URANS simulations. *J. Mar. Sci. Eng.* **2020**, *8*, 355. [CrossRef]
39. Marrone, S.; Colagrossi, A.; Baudry, V.; Le Touzé, D.; Rossi, E. Numerical prediction of extreme loads on flap-type energy converters. In Proceedings of the MARINE 2015-Computational Methods in Marine Engineering VI, Rome, Italy, 15–17 June 2015; pp. 1116–1127.
40. Paduano, B.; Giorgi, G.; Gomes, R.P.; Pasta, E.; Henriques, J.C.; Gato, L.M.; Mattiazzo, G. Experimental validation and comparison of numerical models for the mooring system of a floating wave energy converter. *J. Mar. Sci. Eng.* **2020**, *8*, 565. [CrossRef]
41. Sinamics S120-1FW3 Complete Torque Motors-Configuration Manual 07/2011. Available online: https://cache.industry.siemens.com/dl/files/103/51670103/att_111084/v1/1FW3_en-US.pdf (accessed on 28 October 2021).
42. de Andres, A.; Guanche, R.; Vidal, C.; Losada, I.J. Adaptability of a generic wave energy converter to different climate conditions. *Renew. Energy* **2015**, *78*, 322–333. [CrossRef]